Soil Dynamics and Earthquake Engineering 31 (2011) 1711–1723

Contents lists available at ScienceDirect

Soil Dynamics and Earthquake Engineering

journal homepage: www.elsevier.com/locate/soildyn

Discrete modelling of vertical track–soil coupling for vehicle–track dynamics

G. Kouroussis [a,*], G. Gazetas [b], I. Anastasopoulos [b], C. Conti [a], O. Verlinden [a]

[a] University of Mons – UMONS, Faculty of Engineering, Department of Theoretical Mechanics, Dynamics and Vibrations, Place du Parc 20, B-7000 Mons, Belgium
[b] National Technical University of Athens – NTUA, School of Civil Engineering, Laboratory of Soil Mechanics, Iroon Polytechneiou 9, 15780 Athens, Greece

ARTICLE INFO

Article history:
Received 20 December 2010
Received in revised form
30 May 2011
Accepted 21 July 2011
Available online 10 August 2011

ABSTRACT

This paper presents a coupled lumped mass model (CLM model) for the vertical dynamic coupling of railway track through the soil. The well-known Winkler model and its extensions are analysed and fitted on the result obtained numerically with a finite–infinite element model in order to validate the approach in a preliminary step. A mass–spring–damper system with frequency independent parameters is then proposed for the interaction between the foundations, representing the contact area of the track with the soil. The frequency range of track–soil coupling is typically under 100 Hz. Analytical expressions are derived for calibrating the system model with homogeneous and layered half-spaces. Numerical examples are derived, with emphasis on soil stiffness and layering. The dynamic analysis of a track on various foundation models is compared with a complete track–soil model, showing that the proposed CLM model captures the dynamic interaction of the track with the soil and is reliable to predict the vertical track deflection and the reaction forces acting on the soil surface.

1. Introduction

Dynamic models of railway track are widely used for various applications such as the assessment of stresses on track components, noise emission calculation, or the prediction of ground-borne vibrations. Knothe and Grassie [1] provide a detailed description of these models and a useful classification still applied up to the present time. The assumption of uniform subgrade (railpads and ballast supposed to be continuous along the track) or discrete supports, the adoption of an Euler–bernoulli beam, Timoshenko beam, or a 3D representation define the degree of complexity of the model, depending on the application. For example, the replacement of discrete supports by a continuous layer allows to faithfully to establish the vertical rail deflection solution, whereas the discrete disposition has a non-negligible influence on the definition of the soil loads (sleeper excitation frequency depending on vehicle speed). This particularity has been underlined by Krylov in his ground vibrations prediction model [2].

Another aspect of track modelling is the recognition of the track–soil coupling. Naturally, the dynamic response of the track is largely affected by soil foundation, and track models with rigid foundations cannot be considered accurate. In the case of continuous subgrade, Winkler foundation is totally sufficient. For example, Dieterman and Metrikine [3] propose a continuous model for the rail, using an equivalent elastic foundation for both the ballast and the soil. A forward Fourier transform along the track is adopted to evaluate the coupling between the track and the soil, the latter being modelled as a homogeneous half-space. An equivalent stiffness is derived, showing its dependence on frequency for high-speed loads. Winkler foundation is also used in discrete supports. Zhai and Sun [4] have proposed a detailed model for vertical vehicle–track dynamics, with a complex representation of the ballast, but considering the soil as a Winkler–Voigt foundation. Sarfield et al. [5] and Rücker [6] were the first to study the interaction between the sleepers and the soil through a simple model, without taking into account the ballast. The sleepers were directly connected to the ground, and the importance of such coupling was emphasized for high-speed lines. Analysing the influence of the number of sleeper couplings and soil configuration, Knothe and Wu [7] established that track–soil coupling essentially intervenes in low- and mid-frequency ranges, typically up to 100 Hz. The main conclusion is that the Winkler foundation cannot be used as a half-space model to represent the subgrade in the track model.

Winkler and generalized Winkler models are used however in many geotechnical applications, especially for the dynamic impedance of foundations. Gazetas [8] demonstrated the real efficiency of single degree-of-freedom systems for soil–foundation interaction problems. Advanced representations have been afterwards proposed, as for example the models developed by De Barros and Luco [9], their main difficulty being the identification of model parameters, often performed by fitting results from numerical models or experimental studies. Ju [10] proposed a least-squares

* Corresponding author.
E-mail address: georges.kouroussis@umons.ac.be (G. Kouroussis).

0267-7261/$ - see front matter © 2011 Elsevier Ltd. All rights reserved.
doi:10.1016/j.soildyn.2011.07.007

method for calculating equivalent foundation parameters, using finite element analysis results. In these approximative representations, it is possible however to take into account the effect of nearby sources. Mulliken and Karabalis [11] extended this approach and proposed a discrete system for predicting the dynamic interaction between adjacent rigid surface foundations. As pointed out by the authors, the main difficulty was the modelling of time lag effects associated with wave propagation. A modified Wilson−θ method was proposed for incorporating the coupling between foundations. Time lag is estimated through empirical formulae and is directly included in the integration scheme. More sophisticated models exist, such as Pasternak's model and its extensions. The development follows Winkler's hypothesis, according to which "the deflection at any point on the surface of an elastic continuum is proportional only to the load being applied to the surface, and is independent of the load applied to any other points on the surface" [12]. In addition to the parameters defining the subgrade reaction, supplementary parameters are included for the continuity of adjacent displacements. Various papers (for example [12,13]) present this formulation as an interesting alternative to the simpler foundation models.

All these approaches aim at solving the problem of soil–structure interaction, without the need for excessive computational effort. A calibration is therefore necessary, ideally with the help of analytical or numerical solutions. The finite element method (FEM) provides an interesting alternative to the boundary element method (BEM) and offers the advantage of including complex geometry without difficulty. The main constraint lies in the definition of non-reflecting boundaries at the border of the domain. Recently, Kouroussis et al. [14,15] proposed an efficient 3D model, based on the finite–infinite element method (FIEM). Lysmer's viscous boundaries [16,17] were associated to the infinite elements to increase their efficiency, and to mimic infinity, avoiding reflections at model boundaries. It was shown that the FIEM provides good performance for time domain analysis with small dimensions of the region of interest. Based on this approach, a prediction model for calculating ground vibrations generated by railway traffic was proposed [18]. The track–soil coupling could be incorporated into that numerical approach, but would involve substantial computational effort.

This paper presents a multi-foundation system based on Lysmer's analogue model, with interconnection elements for the foundation-to-foundation coupling. First, the dynamic response of the foundation is analysed, in order to verify the effectiveness of the discrete model in reproducing soil impedance within the range of accuracy required for the track–soil system. For the multi-foundation system, a method is presented for establishing an efficient manner in which to fit the discrete model parameters. The proposed approach is then validated in low frequency where the influence of the subgrade is not negligible. The purpose of the discrete model is to be incorporated in an existing vehicle–track model [18]. Parametric results are produced, with emphasis on soil and ballast stiffness, and soil layering. A computationally efficient simplified representation of the subsoil can therefore be used for vehicle–track dynamics, offering a physical representation of the soil coupling in a track model.

2. Model synopsis

Developing a discrete model for the soil and including it in the vehicle–track model is advantageous for various reasons. The main advantage is the possibility of applying the proposed condensed version of the soil to both time domain and frequency analysis. As it is important to correctly evaluate the forces induced by the vehicle on the rail, the track impedance must be as accurate as possible, taking into account the soil flexibility.

The proposed vehicle–track model is based on a multibody model for the vehicle moving on a flexible track. The latter combines a finite element model for the rail and a lumped mass model for the compound railpads–sleepers–ballast (Fig. 1). Only the vertical motions are studied in this model, so a 2D model is derived for the track. According to [1], this representation is sufficient to predict the rail deflection, to calculate the forces acting on the soil surface, and to evaluate the ground vibrations induced on the neighbourhood by the passing of railway vehicle. Additional information about the modelling can be found in [18].

In order to present a rigorous analysis, vertical track receptances will be studied considering the track on a flexible foundation. These receptances are defined as the frequency response function between the vertical displacement of the rail above a sleeper, and the vertical force applied at the same point or in front of another sleeper. As the FIEM model approach is based on the time domain simulation, the time evolutions of rail motion are also of interest, the decay function being approximated as follows:

$$f_{\text{input}} = \begin{cases} 0 & \text{if } t < t_0 \\ Ae^{[-(t-t_0)/t_d]} & \text{if } t \geq t_0 \end{cases} \quad (1)$$

where parameter A imposes the maximum amplitude and t_d is adjusted to cover an excitation with proper frequency range; $t_0 \neq 0$ for verifying the causality of the response. Track receptances are thus calculated for the time response, using the Fourier transform.

Since railway excitation is often considered small compared to other dynamic excitation (earthquake, explosions, etc.), soil behaviour can reasonably be assumed linear (under the shear strain of 10^{-5}, non-linear behaviour is generally neglected [19]). The domain of ground vibrations and vibratory nuisances is typically in the range 0–80 Hz, according to the DIN standard references [20,21] widely used in the evaluation of vibratory nuisances and discomfort, and of potential stresses induced on structures. For this frequency range, we assume t_0=0.05 s and t_d=0.001 s (the value of A is naturally set to unity). For higher frequencies, t_d can reach up to 0.0001 s.

3. Winkler foundation: state of the art and analysis

The Winkler–Voigt and Lysmer's analogue models are widely used in soil modelling and their effectiveness has been demonstrated through various applications (pile foundation impedance, embedded structure behaviour, etc.). The direct vibrations of a foundation can be represented by a lumped single *dof* system,

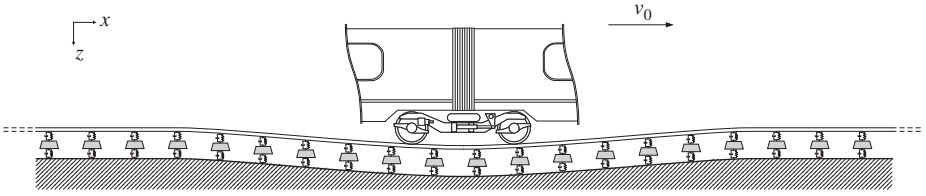

Fig. 1. Vehicle moving on a flexible track.

described by

$$m_f\ddot{x}+d_f\dot{x}+k_f x=f(t), \tag{2}$$

where x represents the motion of the foundation under a vertical load $f(t)$, considering only the vertical vibrations of the foundation. Parameters m_f, k_f and d_f are the equivalent mass, stiffness, and damping of the vertically oscillating system, respectively. The vertical impedance, defined as the ratio of the input force $F(\omega)$ to the foundation response $X(\omega)$, is equal to

$$K_v(\omega)=k_f-\omega^2 m_f+j\omega d_f. \tag{3}$$

The real part here depends on the circular frequency ω, as observed in reality. Notice that parameter m_f does not have any link with the foundation mass.

These parameters can either be fixed, or variable with frequency, according to the model layout representation. If $m_f=0$ and $d_f=0$ and k_f constant, we find Winkler's concept for static reaction. With a non-negative value of d_f, the energy loss is introduced considering a viscoelastic soil behaviour. Parameter m_f allows to adequately account for the variation of the impedance real part with the frequency (Lysmer's analogue model). In a general manner, these parameters require appropriate values, deduced from Young's modulus E, Poisson's ratio ν, density ρ and viscous damping β of the half-space.

Typical results are illustrated in Fig. 2, showing the vertical impedance of a rigid circular massless surface foundation in a viscoelastic homogeneous soil, a layered soil with stiffness increasing with depth, and layered soil with stiffness decreasing with depth, respectively. The last two configurations are simply inverted (last layer characteristics instead of first layer ones, and so on), with extreme Young's moduli E varying from 61 to 465 MPa. The first configuration corresponds to an equivalent homogeneous half-space ($E=146$ MPa). A distinction between the real (in-phase) and imaginary (90° out-of-phase) parts is made, with emphasis on frequency dependency of the dynamic stiffness and the damping coefficient. Besides frequency evolution, the dimensionless frequency:

$$a_0=\frac{\omega R}{c_S} \tag{4}$$

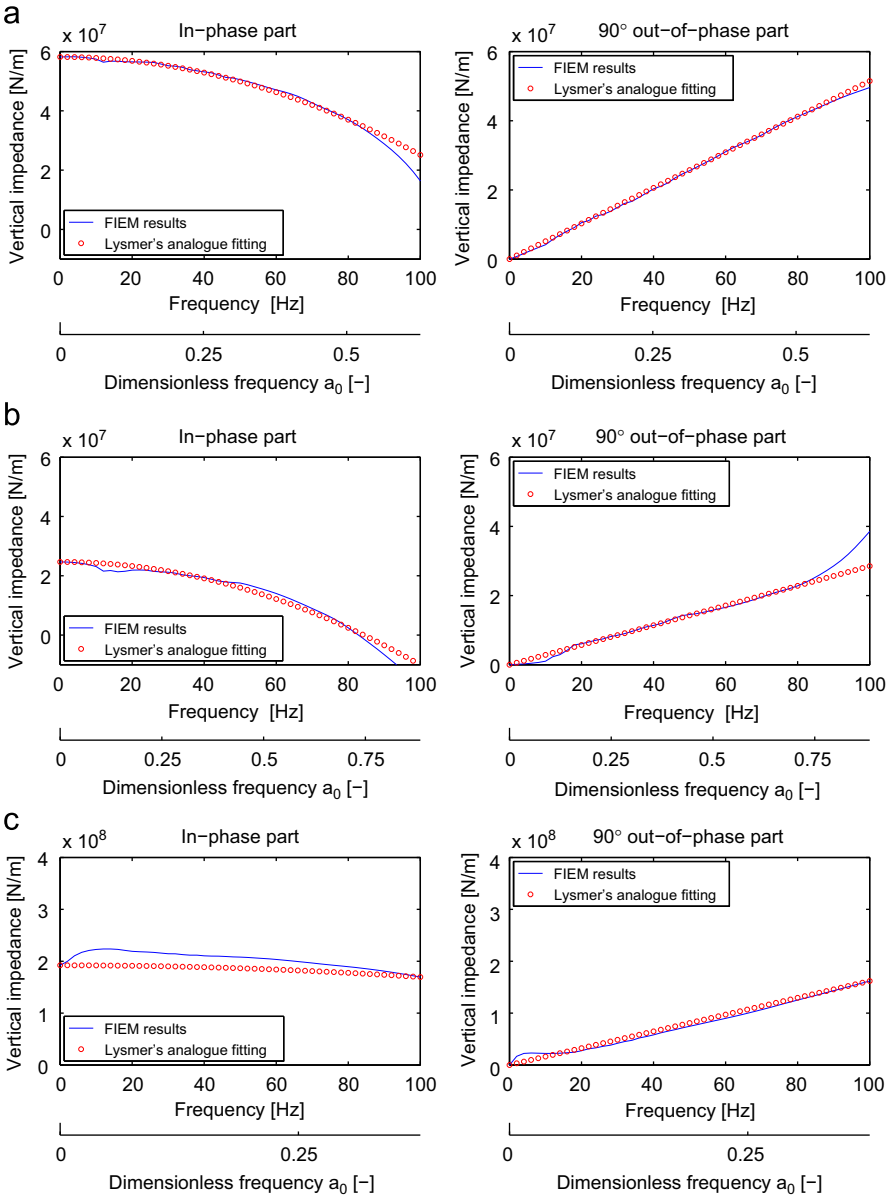

Fig. 2. Comparison between Lysmer's analogue and numerical vertical impedances (circular foundation of radius $R=0.17$ m). (a) Homogeneous soil. (b) Layered soil with stiffness increasing with depth. (c) Layered soil with stiffness decreasing with depth.

is also used to allow the comparison with the literature: dimensionless graphs are often expressed in function of the shear wave velocity c_S (for layered soils, c_S is that of the first layer properties) and of the radius R of the circular rigid foundation. It appears clearly that Lysmer's analogue model can be applied with good accuracy for these configurations: the in-phase curves follow a decreasing second degree parabola with increasing frequency and the out-of-phase curves show a linear evolution ($\Im m[K_v]/\omega$ is nearly perfectly constant). Static stiffnesses can easily be derived, and compared to [8,22]

$$k_f = \frac{2RE}{(1-\nu^2)}. \tag{5}$$

The following observations are noteworthy:

- It appears that the use of "added masses" adequately takes into account the decrease in frequency of stiffness coefficients. Its effect produces dynamic stiffness coefficients of the form $k_f - m_f\omega^2$, for a reasonable approximation for low and medium frequencies.
- Some fluctuations are observed for layered soils, but the general trend remains (Figs. 2(a) and (b)).
- The static stiffness essentially depends on the first layer characteristics.
- At relatively low frequencies, the imaginary part of the impedance is very limited in the second case (Fig. 2(b)) and the real part has the main influence on the impedance function (the phenomenon is described in [8]). For the situation with stiffness decreasing with depth, the imaginary part rapidly increases and reaches up a constant value before following a linear growing (Fig. 2(c)).

The same observations can be made for a rectangular surface $2a \times 2b$ (with $a > b$), and the empirical formula [22]

$$k_f = \frac{Eb}{(1-\nu^2)}\left[1.55\left(\frac{a}{b}\right)^{0.75} + 0.8\right] \tag{6}$$

gives a good estimation of the static stiffness.

4. Coupling between foundations

Having verified the effectiveness of Lysmer's analogue model for reproducing the dynamic impedance of a massless foundation, the formulation is extended to coupled foundations. A coupled lumped mass model (CLM model) is used to determine the relationship between an applied loading function on a rigid foundation attached to an elastic medium, and the corresponding displacement function of the adjacent rigid foundations.

4.1. Multi-foundation coupled lumped mass approach

The proposed model is schematically illustrated in Fig. 3, and consists of discrete masses, springs, and dampers. From the initial Lysmer's analogue model for each foundation (that is to say sleeper-through-the ballast contact area), each foundation is linked with the adjacent ones by springs (parameter k_c) and dampers (parameter d_c). Considering that the force is applied on the ith-element, the equations of motion can be written as

$$m_f\ddot{x}_i + d_f\dot{x}_i + k_f x_i + d_c(\dot{x}_i - \dot{x}_{i-1}) + k_c(x_i - x_{i-1}) + d_c(\dot{x}_i - \dot{x}_{i+1}) + k_c(x_i - x_{i+1}) = f(t), \tag{7}$$

$$m_f\ddot{x}_j + d_f\dot{x}_j + k_f x_j + d_c(\dot{x}_j - \dot{x}_{j-1}) + k_c(x_j - x_{j-1}) + d_c(\dot{x}_j - \dot{x}_{j+1}) + k_c(x_j - x_{j+1}) = 0 \quad (\forall j \neq i). \tag{8}$$

The Fourier transform can be applied, given the following system, if we assume that the index 0 is related to the loaded mass response ($i=0$ and $j=-\infty$ to ∞):

$$\ldots$$

$$[(k_f + 2k_c) - \omega^2 m_f + j\omega(d_f + 2d_c)]X_{-2} - (k_c + j\omega d_c)X_{-3} - (k_c + j\omega d_c)X_{-1} = 0, \tag{9}$$

$$[(k_f + 2k_c) - \omega^2 m_f + j\omega(d_f + 2d_c)]X_{-1} - (k_c + j\omega d_c)X_{-2} - (k_c + j\omega d_c)X_0 = 0, \tag{10}$$

$$[(k_f + 2k_c) - \omega^2 m_f + j\omega(d_f + 2d_c)]X_0 - (k_c + j\omega d_c)X_{-1} - (k_c + j\omega d_c)X_1 = F, \tag{11}$$

$$[(k_f + 2k_c) - \omega^2 m_f + j\omega(d_f + 2d_c)]X_1 - (k_c + j\omega d_c)X_0 - (k_c + j\omega d_c)X_2 = 0, \tag{12}$$

$$[(k_f + 2k_c) - \omega^2 m_f + j\omega(d_f + 2d_c)]X_2 - (k_c + j\omega d_c)X_1 - (k_c + j\omega d_c)X_3 = 0, \ldots \tag{13}$$

where X_j and F represent the spectra of $x_j(t)$ and $f(t)$, respectively. By summing these equations, we obtain

$$[(k_f + 2k_c) - \omega^2 m_f + j\omega(d_f + 2d_c)] \sum_{j=-\infty}^{\infty} X_j - (k_c + j\omega d_c) \times \sum_{j=-\infty}^{\infty} X_j - (k_c + j\omega d_c) \sum_{j=-\infty}^{\infty} X_j = F. \tag{14}$$

The final result appears directly, considering the impedance between all the foundations and the single load acting on a contact area:

$$\frac{F(\omega)}{\sum_{j=-\infty}^{\infty} X_j(\omega)} = k_f - \omega^2 m_f + j\omega d_f. \tag{15}$$

If we suppose that the unloaded responses located far from the input force have a small influence on the total sum of Eq. (14), the latter can be rewritten as

$$\frac{F(\omega)}{\sum_{j=-n}^{n} X_j(\omega)} = k_f - \omega^2 m_f + j\omega d_f, \tag{16}$$

where $2n+1$ is the number of rigid areas that intervene in the coupling ($n=20$ seems to be sufficient). Deriving simple equations, such as Eq. (16), is the key for a rigorous and relatively simple fitting, with emphasis on the properties of the foundations, according to the form of the analytical functions. The same analogy can be made for another function, considering the alternating summation of Eqs. (9)–(13), to obtain the series:

$$[(k_f + 2k_c) - \omega^2 m_f + j\omega(d_f + 2d_c)] \sum_{j=-\infty}^{\infty} (-1)^j X_j + (k_c + j\omega d_c) \times \sum_{j=-\infty}^{\infty} (-1)^j X_j + (k_c + j\omega d_c) \sum_{j=-\infty}^{\infty} (-1)^j X_j = F. \tag{17}$$

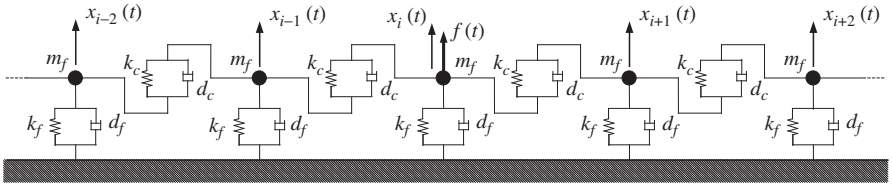

Fig. 3. Multi-foundation model for soil–foundation and foundation-to-foundation interaction.

By limiting the number of terms to $2n+1$, we finally obtain

$$\frac{F(\omega)}{\sum_{j=-n}^{n}(-1)^j X_j(\omega)} = (k_f+4k_c)-\omega^2 m_f + j\omega(d_f+4d_c). \tag{18}$$

Notice that, due to the symmetry of the problem,

$$\sum_{j=-n}^{n} X_j(\omega) = X_0(\omega)+2\sum_{j=1}^{n} X_j(\omega) \tag{19}$$

$$\sum_{j=-n}^{n} (-1)^j X_j(\omega) = X_0(\omega)+2\sum_{j=1}^{n} (-1)^j X_j(\omega) \tag{20}$$

only one side of contact area set can be investigated.

Parameters can be easily updated from a numerical model, in this instance a 3D FIEM model, considering a quadratic function for real parts and a linear function for the imaginary one, for both Eqs. (16) and (18), as far as the numerical responses follow these specific curves. In particular, k_f and k_f+4k_c represent the static component of the total sum and the alternating summation, respectively.

4.2. Particularity of the cross damping coefficient

To estimate the time lag, Mulliken and Karabalis [11] have proposed a formula initially available for square foundations. Applied to rectangular $2a \times 2b$ foundations, this formula gives a good estimation of the time delay:

$$\tau = \frac{3}{4}\frac{(d+b/2)}{c_S} \tag{21}$$

with d the sleeper spacing and c_S the shear wave velocity (τ is around 0.003–0.004 s in most typical railway/soil configurations). In order to avoid procedures for adding the time lag, due to wave propagation in the soil, directly to the numerical scheme, analyses have been conducted that show that the damping term d_c can be negative.

Let us consider a part of the CLM model (Fig. 4) represented by the damped 1–*dof* model, with the spring k_f, the damper d_f and the mass m_f for the foundation, and the spring k_c and the damper d_c for the coupling between foundations. The displacement of the two foundations is described by x_1 and x_2. The transmissibility function between these two displacements can be written as

$$\frac{X_2}{X_1} = \frac{k_c+j\omega d_c}{(k_f+k_c)-\omega^2 m_f + j\omega(d_f+d_c)}. \tag{22}$$

The term $j\omega(d_f+d_c)$ in the denominator plays the role of phase lag and the term $j\omega d_c$ in the numerator is related to a phase lead. The analysis of Eq. (16) essentially imposes the values of k_f, d_f and m_f. In soil motion, the time lag is non-negligible and the value of d_f could not be sufficient. It appears that an additional delay is introduced by a negative damper d_c into the system, transforming the time lead to an additional time lag. Impedance defined by Eq. (18) is used to adjust the other parameters, and it reveals this particularity of d_c. At low circular frequencies, the delay induced by d_c value can be estimated by

$$\tau_c = -d_c\left(\frac{1}{k_c}-\frac{1}{k_c+k_f}\right). \tag{23}$$

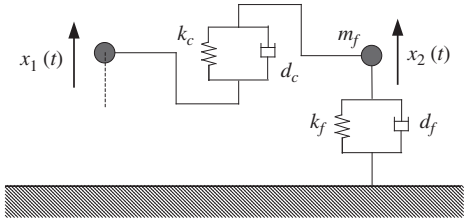

Fig. 4. Two-foundation model for soil interaction.

When structural damping is considered in the multi-foundation system, the global dashpot term d_c contains the contribution of the delay and also the contribution of the material damping existing between the two contact areas, and may be negative. A condition to avoid instability is to verify that the damping matrix of the whole system is positive definite. If the negative damping is larger than the inherent structural damping, the response will naturally diverge. Therefore, as the distance d representing the sleeper bay is small (0.60–0.72 m), the damping d_c magnitude will generally be small. For larger distances, a divergence inevitably appears.

4.3. Parametric analysis

Before applying any fitting between this model and a numerical model (in this case, the FIEM model), a sensitivity analysis is performed. Fig. 5 displays the results obtained with an excitation defined by Eq. (1) by varying, one parameter at a time, the stiffnesses k_f and k_c, the damping coefficients d_f and d_c, and the mass m_f, plotting time histories and soil receptances (loaded surface and second unloaded surface), and also the maximum amplitude with the distance.

Several comments can be made on each parameter, as far as the results shown in these figures are concerned:

- The mass m_f has an obvious influence on the resonance frequency, which can be approximated by

$$f_R = \frac{1}{2\pi}\sqrt{\frac{k_f+2k_c}{m_f}}. \tag{24}$$

  The maximum amplitude is identical for the loaded surface in all cases. However, the maximum amplitude level with the distance increases as mass increases. From these results (1st row, 2nd column), there seems to be a time lag with greater mass.
- The decrease in foundation stiffness k_f induces an increase in maximum amplitude with distance. The static stiffness of each response obviously diminishes. The time signal seems to be "amplified" when stiffness values are small, the effect being more pronounced with the distance.
- The foundation damping d_f has a strong influence on the maximum amplitude, increasing it equally whatever the distance. Each signal is also damped, with a limit of stability (here d_f=800 kN s/m) with a negative d_c imposed.
- The coupling stiffness k_c also affects the maximum amplitude of the signal. For the loaded and the first unloaded surfaces, the more important the stiffness is, the more the amplitude level diminishes. For the further surfaces, it is the opposite effect. The time lag is imposed by this parameter if the damping d_c is fixed (see Eq. (23)).
- The maximum amplitude is almost independent of the damping d_c. Here also a limit of stability exists.

5. Numerical example

To validate the proposed model, the track receptance is calculated in various cases, as it gives a picture of the rail head displacement where a force (typically the vehicle loads) acts on a rail point. The flexible rail, defined by its Young modulus E_r, geometrical moment of inertia I_r, area A_r and density ρ_r, is described by the finite element method. A regular spacing d of the sleepers (of mass m) has been considered. Railpads and ballast are modelled by

springs and dampers : k_p and d_p for the railpad, k_b and d_b for the ballast. The soil condensed form is added under the track, as presented in Fig. 6, with the parameters m_f, k_f, k_c, d_f and d_c.

Track receptances $H_{i1}(\omega)$ are related to the excitation $f(t)$ applied on the rail at point 1 and the responses at point i (from 5′ to 5 in the diagram of Fig. 6). Due to the finite length of the track (bounded track), the modelling must be done with caution to avoid border effects, as highlighted by Knothe and Wu [7], who confirm that five sleepers on both sides intervene in the rail deflection. To be sure, a minimum of 10 sleepers is necessary on both sides of the region of interest (length of the track sufficient to avoid any interference due to the extremities of the rail). On the other hand,

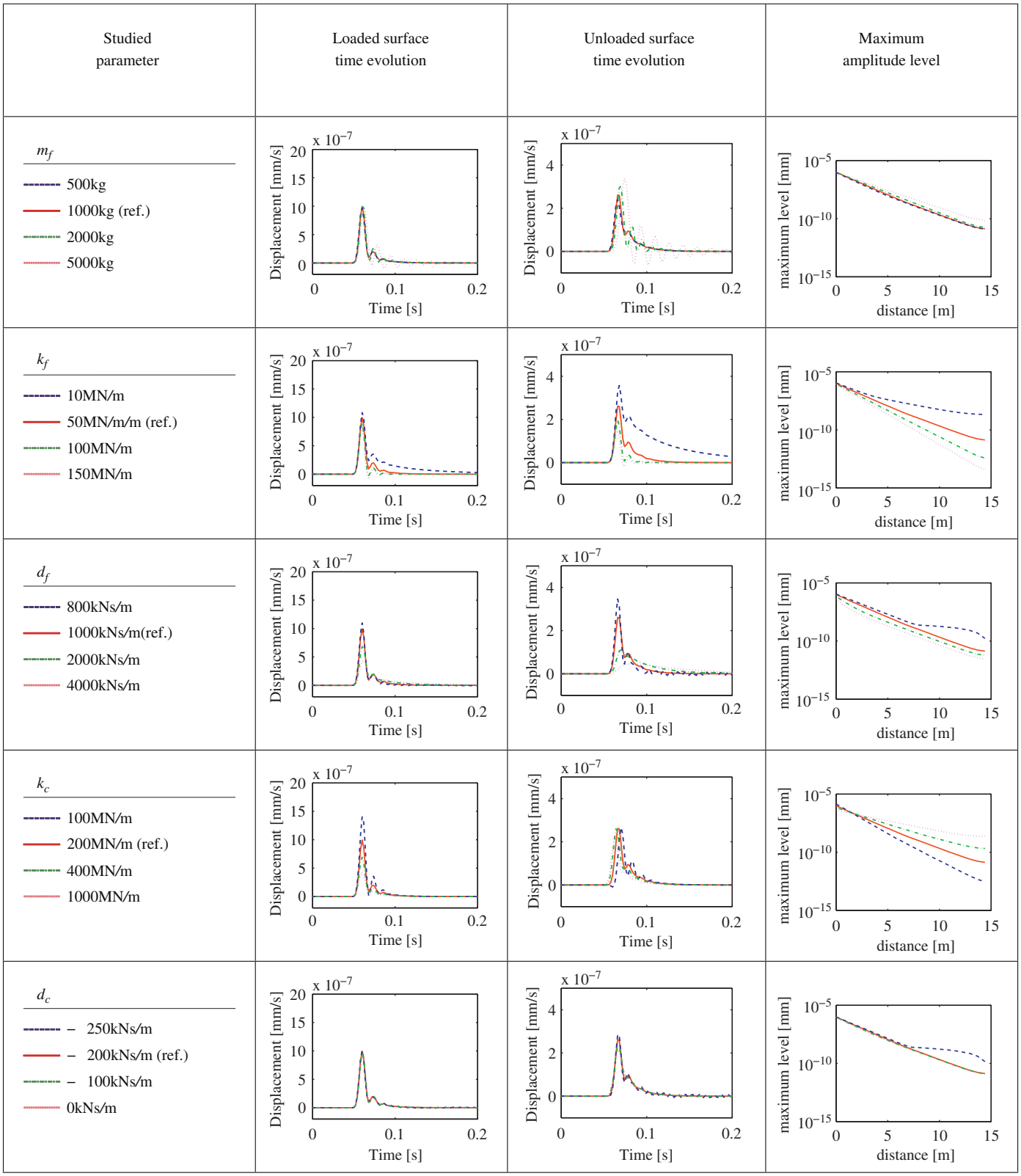

Fig. 5. Summary of the parametric study results.

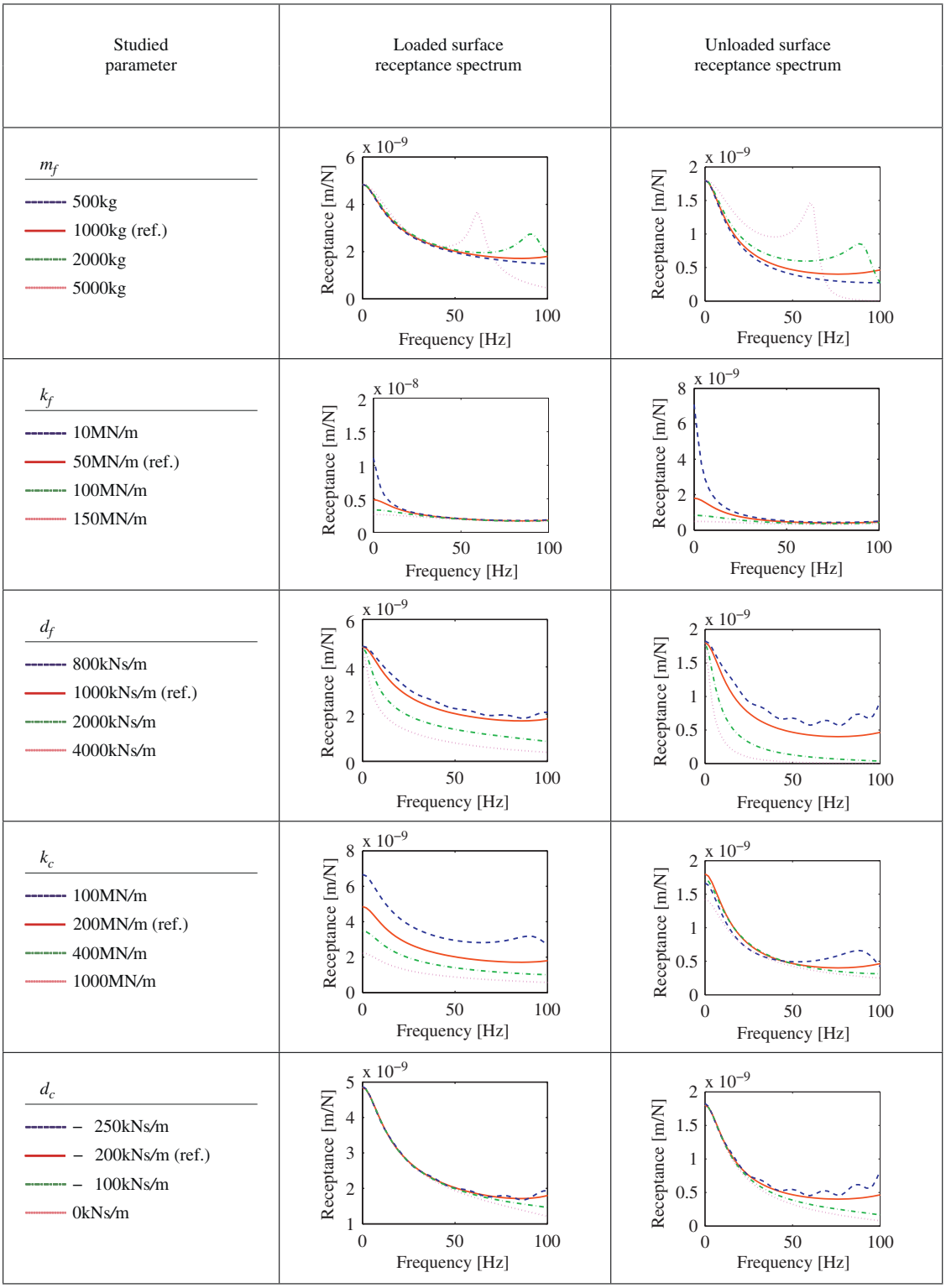

Fig. 5. (*continued*)

the discretisation is less restrictive and two beam elements by sleeper bay are sufficient to model track dynamics [23].

For the validation, a numerical model is established, based on the track coupled with a numerical model of the soil (the ballast links the sleepers and the soil surfaces completely). The soil is modelled with the FIEM approach, according to [14], and the ballast reactions are applied directly on a rectangular rigid surface representing the sleeper area.

5.1. Validation on a typical example

The first example is based on a homogeneous half-space. Dynamic parameters are presented in Table 1, as well as the discrete CLM model parameters obtained from the calibration presented in Section 4. This configuration corresponds to a Belgian site investigated in the past (at Mévergnies, along the high-speed line Brussels–Paris/London and near the French border).

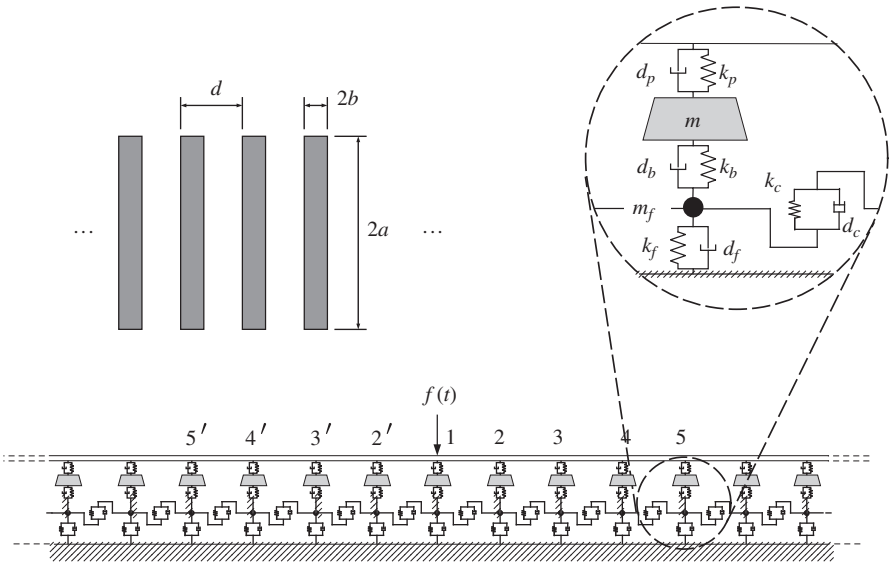

Fig. 6. The flexible track model, taking account of the condensed soil.

Table 1
Mévergnies site (Belgium)—half-space configuration.

E	ρ	ν	c_P	c_S	β
129 MPa	1600 kg/m^3	0.3	330 m/s	177 m/s	0.0004 s
m_f	d_f	k_f	d_c	k_c	
380 kg	680 kN s/m	72 MN/m	−155 kN s/m	160 MN/m	

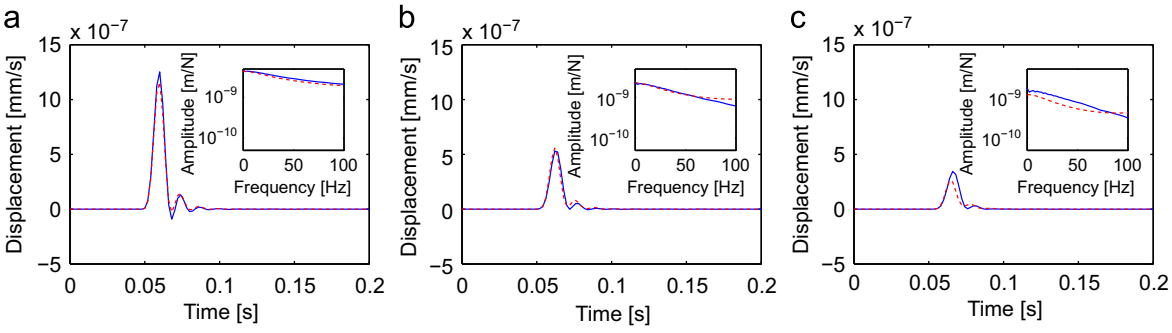

Fig. 7. Comparison between coupled lumped mass model (dashed line) and FIEM numerical results (solid line) for a typical half-space. (a) Time evolution (loaded surface). (b) Time evolution (unloaded surface—1st). (c) Time evolution (unloaded surface—2nd).

Fig. 7 presents a preliminary result, considering the vibrations of the first five rectangular contact areas (the loaded area and the two adjacent ones on each side) and based on the comparison of the soil motions in both models when the force (1) acts directly on the rectangular ground surface 2.5 m × 0.285 m. Excellent agreement is observed between the simplified model and the rigorous one, especially for the area near the excitation. It would be ideal and optimistic to find a perfect correspondence for all the contact areas. It is well known that the nearby surfaces play the major role on the coupling, as expected by Rücker [6]. It seems that very good estimates of the vertical stiffness and coupling of soil modelling can be made by the CLM model.

Adding the track on this soil representation (Table 2), the track receptance can be calculated. Fig. 8 displays the results in terms of amplitude and phase, for the direct receptance H_{11} and the two indirect receptances H_{21} and H_{31}, up to 350 Hz. Two resonances appear in the curve, in accordance with the track modelling: the first, around 65 Hz, corresponds to the vertical motion where the rail and sleepers vibrate in-phase. The second, at 325 Hz, corresponds to the vertical motion where rail and sleepers mainly vibrate out-of-phase. The developed CLM model gives results very close to the numerical ones, with an undeniable benefit in computational time (a reduction of more than 90%).

5.2. Validation for soft soil

The second validation concerns the influence of the stiffness of the soil, compared to that of the track. Obviously, the track stiffness, and more particularly its ratio to soil stiffness plays an important role in the track receptance curves. The following analysis allows to establish its influence by varying the soil stiffness: $E=10$, 155 and 750 MN/m^2 for soft, medium, and stiff soil, respectively. The other parameters are set at $\rho=1540$ kg/m^3, $\nu=0.25$ and $\beta=0.0004$ s. Table 3 gives the correspondence between the soil dynamic parameters and those related to the CLM model (coupled lumped model).

The results are compared also with those obtained for track on Lysmer's analogue foundation (uncoupled lumped model). The railpad and ballast parameters are slightly different from those in the previous example ($k_p = 90$ MN/m, $d_p = 30$ kN s/m, $k_b = 120$ MN/m, $d_b = 40$ kN s/m) with a sleeper spacing $d = 0.72$ m. In this case, vertical track resonance frequencies are 124 and 289 Hz. This configuration allows to stress the low frequencies by amplifying the first resonance to the detriment of the second one.

Table 2
Parameters of the track of Mévergnies.

E_r	I_r	ρ_r	A_r	d
210 GPa	3055 cm^4	7850 kg/m^3	76.9 cm^2	0.6 m
k_p	d_p	k_b	d_b	m
120 MN/m	4 kN s/m	47 MN/m	72 kN s/m	150 kg

Fig. 9 presents the expected results for the direct receptance H_{11} and the adjacent indirect receptance H_{21}. The model with Lysmer's analogue foundation is accurate for stiff soil (compared to the ballast stiffness) only (difference less than 0.5 dB). This explains why the hypothesis of track–soil decoupling proposed by Kouroussis et al. [18] is only valid if the foundation stiffness k_f is sufficient compared to that of the ballast:

$$\frac{1}{k_b} + \frac{1}{k_f} \approx \frac{1}{k_b}. \tag{25}$$

The CLM model provides better results. For medium soil (Fig. 9(b)), the difference is negligible (as was the case in the preceding validation step). In the case of soft soil (Fig. 9(a)), the following points are noteworthy:

- The coupling strongly attenuates the differences observed with Lysmer's analogue foundation (from initially 20 dB up to 4 dB in the receptance amplitude).

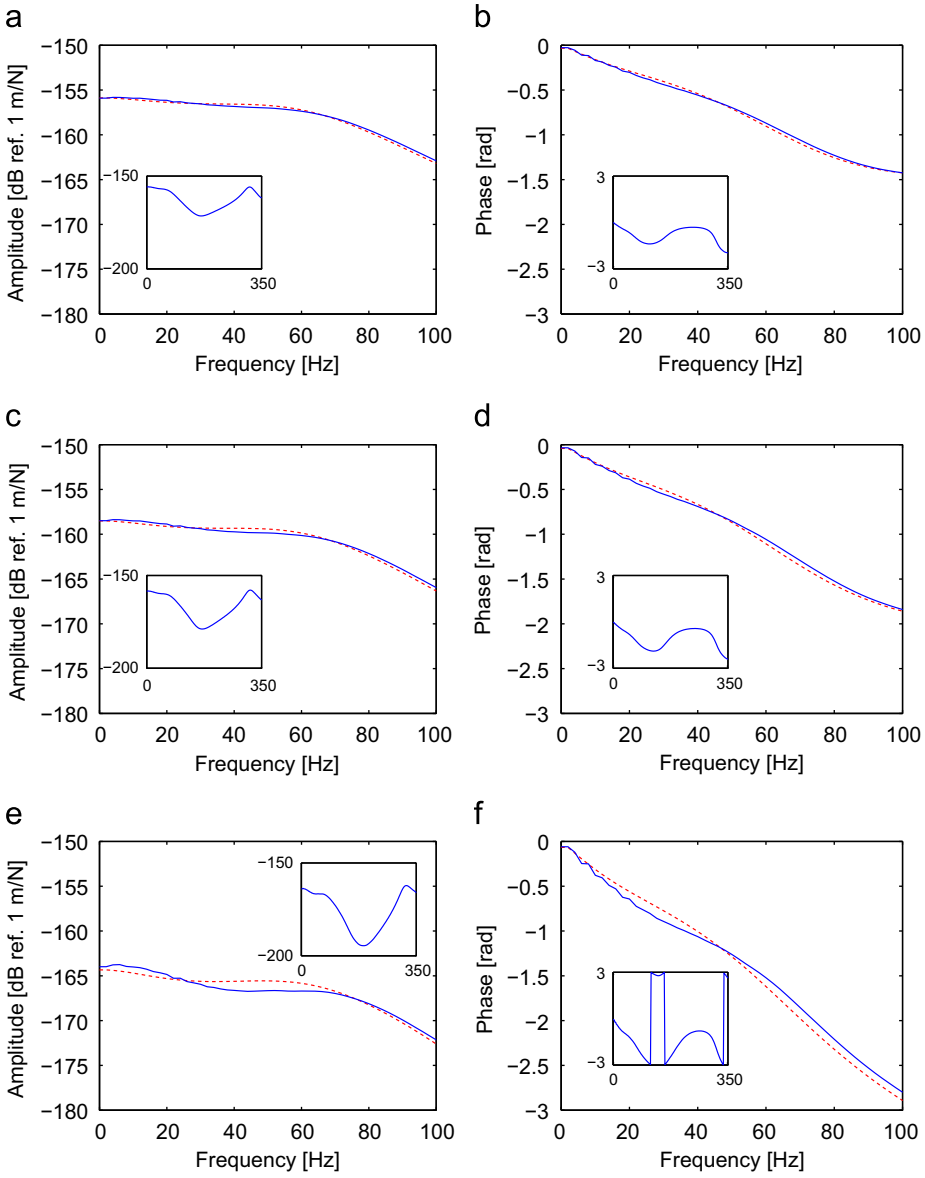

Fig. 8. Track receptances amplitude (left) and phase (right) for the site of Mévergnies (homogeneous case). Comparison of CLM model (dashed lines) with rigorous FEM model (solid lines). (a) Amplitude—in front of sleeper 1. (b) Phase—in front of sleeper 1. (c) Amplitude—in front of sleeper 2. (d) Phase—in front of sleeper 2. (e) Amplitude—in front of sleeper 3. (f) Phase—in front of sleeper 3.

- Under 10 Hz, no difference appears with the FIEM results. In particular, the static stiffness is accurately captured. The decrease in amplitude with frequency in this frequency range is also captured while Lysmer's analogue foundation model fails to predict this trend. Up to 50 Hz, the difference in amplitude is negligible.

5.3. Validation for various ballast stiffness

The ballast stiffness also plays a role in the track receptance and in the track–soil coupling. The soil stiffness is imposed here at 155 MN/m^2 and three values are chosen for the ballast stiffness: k_b=50 MN/m, k_b=120 MN/m and k_b=600 MN/m. The other track and soil parameters are identical to the preceding ones. The first vertical track resonance frequency varies from 82 Hz to 228 Hz.

Table 3
Coupled lumped mass model parameters for various soil.

Studied case (MN/m^2)	m_f (kg)	d_f (kN s/m)	k_f (MN/m)	d_c (kN s/m)	k_c (MN/m)
Medium soil (E=155)	758	1120	69	−218	157
Hard soil (E=750)	1396	2550	317	−300	724
Soft soil (E=10)	94	180	5	−30	15

Fig. 10 shows the track receptances for each case and allows to compare configurations between each other. The difference between FIEM model and CLM model results is clearly low in the frequency range concerned by track–soil coupling (0–100 Hz). These analyses validate the use of the approximated model for a large ballast stiffness range, compared to classical track models without considering the soil influence. These models can present a difference reaching up to 10 dB, despite of a medium soil configuration. For all cases, the approximation is very good compared to the receptances calculated for a Lysmer's analogue foundation.

The above results show that the proposed CLM model successfully predicts the track–soil dynamic behaviour, for any track (ballast) stiffness. The next section deals with model validation for layered soil.

5.4. Validation for layered soil

The layered configuration proposed in Section 3 is presented in detail in Table 4. An advanced soil configuration is proposed, based on the analysis performed by Degrande et al. [24] for a railway site in Brussels.

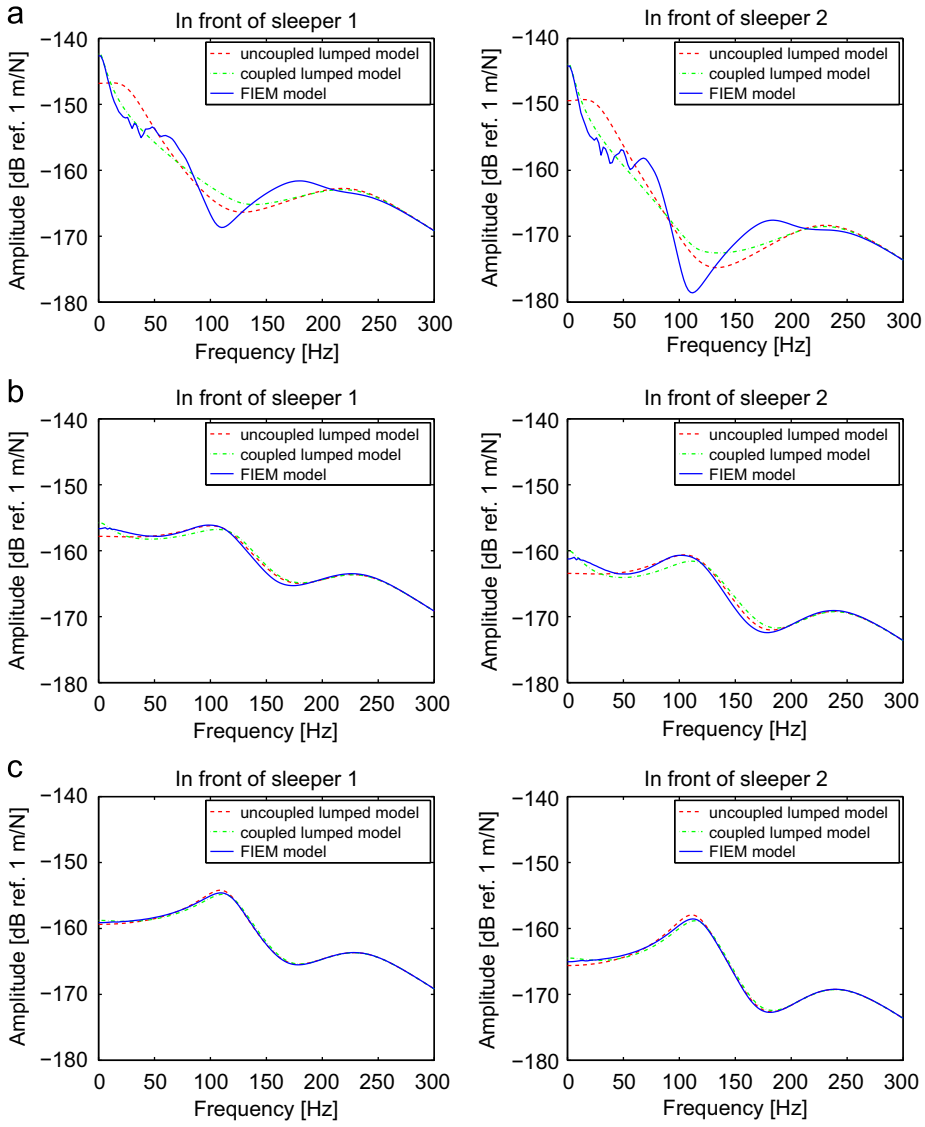

Fig. 9. Direct (left) and indirect (right) track receptances for: (a) soft soil (E=10 MN/m^2), (b) medium soil (E=155 MN/m^2), and (c) stiff soil (E=750 MN/m^2).

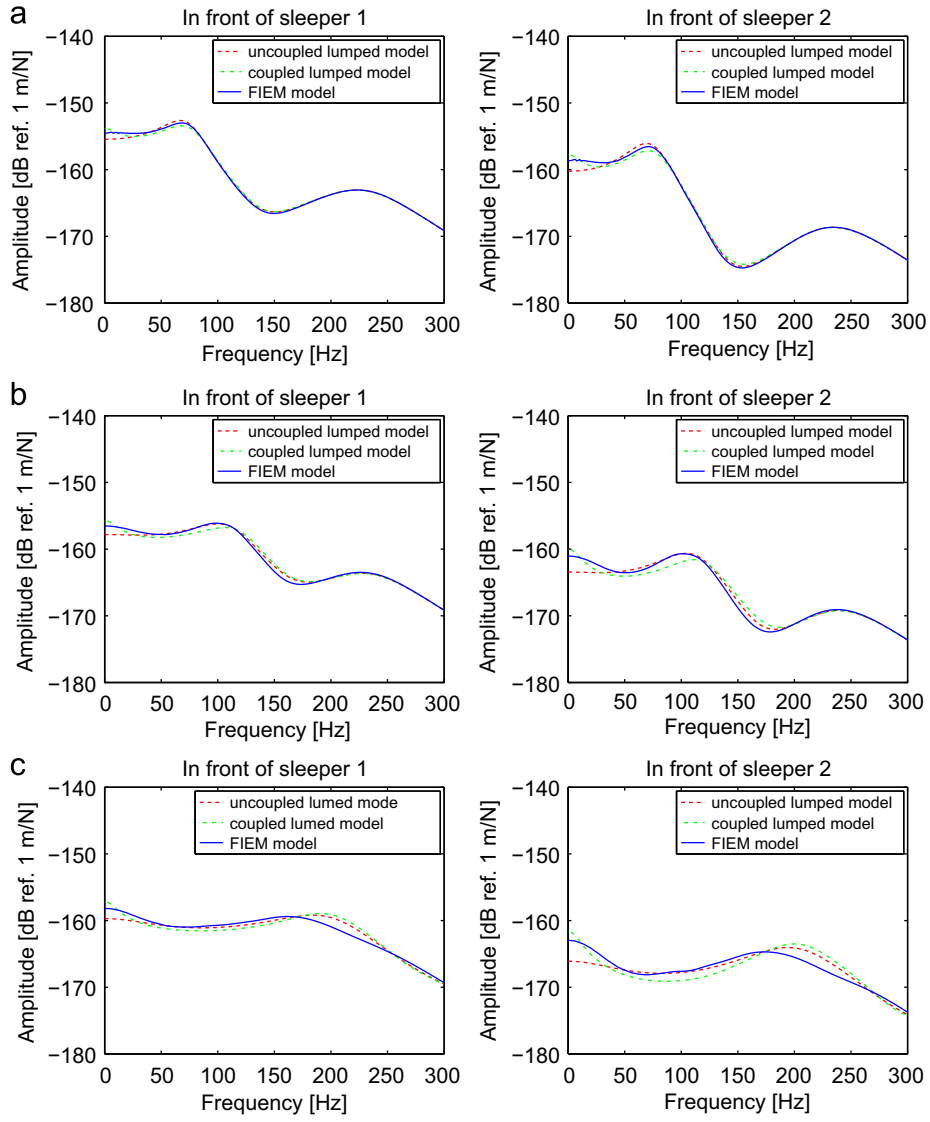

Fig. 10. Direct (left) and indirect (right) track receptances for: (a) soft ballast (k_b=50 MN/m), (b) medium ballast (k_b=120 MN/m), and (c) stiff ballast (k_b=600 MN/m).

Table 4
Haren site (Belgium)—layered soil case.

Layer	d	E (MPa)	ρ (kg/m^3)	ν	c_P (m/s)	c_S (m/s)	β (s)
1	1.2	61	1876	0.13	184	120	0.0004
2	1.8 m	84	1876	0.13	215	170	0.0004
3	1.0 m	287	1876	0.13	400	260	0.0004
4	1.0 m	373	1876	0.27	500	280	0.0004
5	1.0 m	450	1876	0.33	600	300	0.0004
6	∞	465	1992	0.48	1458	286	0.0004

m_f	d_f	k_f	d_c	k_c
5003 kg	300 kN s/m	60 MN/m	−45 kN s/m	81 MN/m

Fig. 11 presents the results of the validation, including the prediction using Lysmer's analogue model for the foundation. This results addition allows to quantify the gain brought by the foundation coupling in the approximated model. Here, we do not only consider the indirect receptance of the rail point in front of the adjacent sleeper, but also the other points up to the fifth sleeper. The first vertical track resonance frequency is around 70 Hz. The most significant discrepancies between models appears in the case of layered configuration, where it is sometimes difficult to adjust the parameters in order to recover the soil resonances (here around 15 Hz and 40 Hz), otherwise easily calculated by [25]

$$f_{k,n} = (2n-1)\frac{c_k}{4d} \tag{26}$$

where k subscript is related to the body waves (P or S) of the upper layers. In the case of n=1 and for P-waves, this resonance

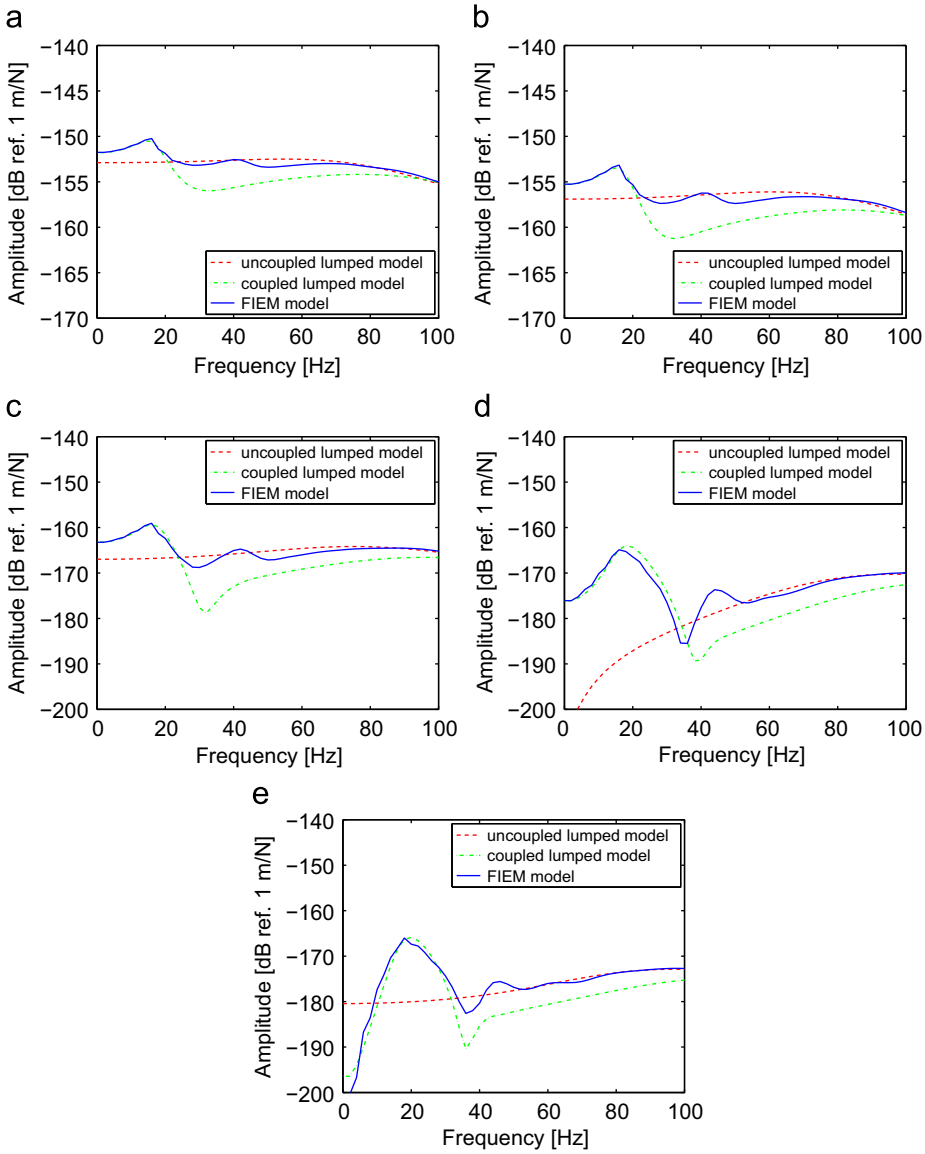

Fig. 11. Direct and indirect track receptances for the site of Haren (layered case). (a) In front of sleeper 1. (b) In front of sleeper 2. (c) In front of sleeper 3. (d) In front of sleeper 4. (e) In front of sleeper 5.

frequency corresponds to the natural oscillation frequency of free vertical response of the soil surface [8]. Results show that the CLM model predicts the first resonance accurately. In all curves, the static stiffness for each rail point is well represented by the CLM model; the simple model (Lysmer's analogue foundation) is less accurate. It appears that, if we progressively move away from the applied load (in front of sleepers 4 and 5), the amplitude level strongly diminishes. Difference for points far from the load seems to be more important, but the amplitude is approximately 20 dB smaller than for the direct case. The influence is therefore negligible.

6. Conclusions

An efficient discrete model for track/soil coupling is proposed, as an extension of the well-known Lysmer's analogue model. A first step consisted in analysing the efficiency of the discrete single degree-of-freedom model, comparing the vertical impedance with equivalent numerical solutions, and showed that very good results can be obtained by these models for ballast–soil interaction. Compared to Winkler's model, adding an equivalent mass allows to consider the part of the soil mass that participates in the foundation vibration.

An alternative to Lysmer's analogue model has been proposed, considering the coupling between foundations, in terms of their contact surface areas. The coupled lumped mass model (CLM model) of n degrees of freedom considers the coupling between all the sleeper areas by interconnecting them with springs and dampers.

The key conclusions can be summarized as follows:

- The fitting is proposed through simple analytical relations like those related for the Lysmer's analogue model (quadratic frequency evolution of the real part and linear evolution for the imaginary one). A parametric study was performed to adjust some parameters for better calibration.
- Very good results are obtained by fitting the CLM model with numerical results obtained by the FIEM modelling of the soil, in various cases (homogeneous soil and layered media) in the frequency range 0–80 Hz.
- The soil wave propagation induces non-negligible time lag, which can be assessed with a negative dashpot term placed

between the masses. By adding the structural damping, the stability of the integration scheme is preserved if small distances are considered (which is the case of railway track).

The proposed model, associated to a track model, has been validated in various ballast and soil conditions, considering ballast and soil flexibility, and soil layering. Good agreement with rigorous FIEM results was obtained.

References

[1] Knothe K, Grassie SL. Modelling of railway track and vehicle/track interaction at high frequencies. Vehicle System Dynamics 1993;22:209–62.

[2] Krylov VV. Effect of track properties on ground vibrations generated by high-speed trains. Acustica—Acta Acustica 1998;84(1):78–90.

[3] Dieterman HA, Metrikine AV. The equivalent stiffness of a half-space interacting with a beam, critical velocities of a moving load along the beam. European Journal of Mechanics A/Solids 1996;15(1):67–90.

[4] Zhai W, Sun X. A detailed model for investigating vertical interaction between railway vehicle and track. Vehicle System Dynamics 1994;23(supplement): 603–15.

[5] Sarfeld W, Savidis SA, Schuppe R, Klapperich H. Three-dimensional dynamic interaction of ties. In: Xth ICSMFE (Internationale Baugrundtagung), vol. 3, Stockholm (Sweden); 1981. p. 287–92.

[6] Rücker W. Dynamic interaction of a railroad–bed with the subsoil. In: Soil dynamics & earthquake engineering conference, vol. 2, Southampton, England; 1982. p. 435–48.

[7] Knothe K, Wu Y. Receptance behaviour of railway track and subgrade. Archive of Applied Mechanics 1998;68:457–70.

[8] Gazetas G. Analysis of machine foundation vibrations: state of the art. Soil Dynamics and Earthquake Engineering 1983;2(1):2–42.

[9] De Barros FCP, Luco JE. Discrete models for vertical vibrations of surface and embedded foundations. Earthquake Engineering & Structural Dynamics 1990;19(2):289–303.

[10] Ju SH. Evaluating foundation mass, damping and stiffness by the least-squares method. Earthquake Engineering & Structural Dynamics 2003;32(9): 1431–42.

[11] Mulliken J, Karabalis D. Discrete model for dynamic through-the-soil coupling of 3-D foundations and structures. Earthquake Engineering & Structural Dynamics 1998;27(7):687–710.

[12] Tanahashi H. Pasternak model formulation of elastic displacements in the case of a rigid circular foundation. Journal of Asian Architecture and Building Engineering 2007;173:167–73.

[13] Jones R, Xenophontos J. On the Vlasov and Kerr foundation models. Acta Mechanica 1976;25:45–9.

[14] Kouroussis G, Verlinden O, Conti C. Ground propagation of vibrations from railway vehicles using a finite/infinite-element model of the soil. Proceedings of the IMechE, Part F: Journal of Rail and Rapid Transit 2009;223(F4):405–13.

[15] Kouroussis G, Verlinden O, Conti C. Efficiency of the viscous boundary for time domain simulation of railway ground vibration. In: 17th international congress on sound and vibration (ICSV17), Cairo, Egypt; 2010.

[16] Lysmer J, Kuhlemeyer RL. Finite dynamic model for infinite media. Journal of the Engineering Mechanics Division, Proceedings of the ASCE 1969;95(EM4): 859–77.

[17] Kouroussis G, Verlinden O, Conti C. Finite-dynamic model for infinite media: corrected solution of viscous boundary efficiency. Journal of Engineering Mechanics 2011;137(7):509–11.

[18] Kouroussis G, Verlinden O, Conti C. On the interest of integrating vehicle dynamics for the ground propagation of vibrations: the case of urban railway traffic. Vehicle System Dynamics 2010;48(12):1553–71.

[19] Schevenels M. The impact of incertain dynamic soil characteristics on the prediction of the ground vibrations. PhD thesis, Katholieke Universiteit te Leuven; 2007.

[20] Deutsches Institut für Normung. DIN 4150-2: structural vibrations—part 2: human exposure to vibration in buildings; 1999.

[21] Deutsches Institut für Normung. DIN 4150-3: structural vibrations—part 3: effects of vibration on structures; 1999.

[22] Wolf JP. Foundation vibration analysis using simple physical models. New Jersey, USA: Prentice–Hall; 1994.

[23] Kouroussis G, Verlinden O, Conti C. Complete vehicle/track/soil modelling for the prediction of its environmental impact. In: ITT'09 symposium on technological innovation & transport systems, Paris, France; 2009.

[24] Degrande G, De Roeck G, Dewulf W, Van den Broeck P, Verlinden M. Design of a vibration isolating screen. In: Sas P, editor. Proceedings ISMA 21, noise and vibration engineering, vol. II. Leuven, Belgium; 1996. p. 823–34.

[25] Lefeuve-Mesgouez G, Peplow AT, Le Houédec D. Surface vibration due to a sequence of high speed moving harmonic rectangular loads. Soil Dynamics and Earthquake Engineering 2002;22(6):459–73.